

The ACT bridge census: a search for hot gas between massive galaxy clusters with pair stacking

G. Isopi^{1,2,3,*} for the ACT collaboration

¹Dipartimento di Fisica, Sapienza Università di Roma, Piazzale Aldo Moro, 5, 00185, Rome (RM), Italy

²INFN Sezione Roma1, Piazzale Aldo Moro, 2, 00185, Rome (RM), Italy

³INAF OAC, Via della Scienza, 5, 09047, Selargius (CA), Italy

Abstract. Baryonic matter only accounts for 5% of the mass-energy density of our universe, where the other 95% is shared between dark energy and dark matter. Measurements of the early universe predict a certain baryon fraction, that is not detected in the later stages of the cosmic evolution, and this discrepancy between predicted and observed baryons is known as the “missing baryon” problem. Cosmological simulations predict that a significant fraction of the missing baryons could be found in the form of the warm-hot intergalactic medium (WHIM) trapped inside large scale structures that constitute the cosmic web. WHIM can be detected using the thermal Sunyaev-Zel’dovich effect, as the amplitude of its spectral distortion scales linearly with the electron pressure integrated along the line of sight. This effect has been extensively used by space and ground based CMB experiments to study clusters and filament candidates. In this work, we present results on the detection of hot gas between pairs of candidate interacting galaxy clusters obtained with the latest high resolution (1.65’), high sensitivity Compton- γ maps from ACT. We consider a set of candidate double cluster systems extracted from a preliminary ACT-DR6 catalog of clusters blindly detected with a matched filter approach. We then aligned and stacked these cluster pairs in order to increase the SNR and detect the faint SZ signal due to warm-hot filaments of gas connecting them. This sample focuses on short filaments with a projected length $\ell_{fil} < 10$ Mpc and typical halo mass $M_{500} \sim 2 \times 10^{14} M_{\odot}$. Additionally, we study individual pairs of clusters to identify promising candidates for follow-up observations using higher (10 – 20”) resolution millimeter cameras or X-ray satellites.

1 Introduction

The Λ CDM model currently represent the best description we have of the evolution of our universe. With only seven parameters, it is able to predict with very high accuracy a plethora of observables, spanning from temperature and polarization anisotropies of the cosmic microwave background (CMB), to the assembly of matter on the largest scales, namely the large scale structure (LSS) of the universe, and the relative abundance of baryonic matter with respect to the dark matter and dark energy components. Early universe measurements show that the baryons account for about 5% of the mass-energy density of the universe, while the

*e-mail: giovanni.isopi@uniroma1.it

other 95% is dominated by the dark component [1–3]. The baryon abundance inferred from fast radio burst dispersion measurements ($z \approx 0.5$) is consistent with the value from CMB estimates ($z \approx 1100$), supporting the evidence that the baryon fraction has remained constant through the cosmic age. Another method to measure the baryon fraction in the late universe is to measure the amount of matter in different environments and add all the contributions. In Fukujita *et al.* (1998) [4], this calculation shown that the amount of baryons contained in galaxies and in the intra-cluster medium (ICM) of galaxy clusters was much smaller than the early universe abundance. This discrepancy was named "missing baryons problem". Later works based on simulations (see, e.g., [5]) proposed that most of the baryons are located outside galaxy clusters, in a low density, low temperature state named warm-hot intergalactic medium (WHIM), trapped in the potential wells of the large scale structures of the universe known as the cosmic web. In these conditions of low temperature and density, the X-ray luminosity is rather low, making these baryons relatively difficult to detect. For instance, filaments show a density $10^2 - 10^3$ times lower than clusters, and since the X-ray bremsstrahlung emission scales as n_e^2 , their surface brightness is several orders of magnitude fainter than clusters. Baryons in the late universe are therefore undetected, rather than "missing", as supported by fast radio bursts (FRBs) measurements.

An useful tool to detect baryons outside galaxy clusters is the thermal Sunyaev-Zel'dovich effect (tSZ) [6–8]. This effect arises from the inverse Compton scattering of cold CMB photons with hot electrons typically found in galaxy clusters or in the structures of the cosmic web. The scattering process increases the energy of the photons, which are up-scattered from low frequencies to higher frequencies. Since the photon number is conserved in this scattering process, the effect is that a cloud of hot electrons, like a cluster, is observed as a cold spot at frequencies below 217 GHz and as a hot spot at higher frequencies. The amplitude of the tSZ, in the non-relativistic regime, is given by the Compton- y parameter, that is proportional to the electron pressure integrated along the line of sight [6]:

$$y = \frac{\sigma_T}{m_e c^2} \int k_B n_e(\ell) T_e(\ell) d\ell, \quad (1)$$

Taking advantage of the component separation methods typically used for separating the CMB signal from foregrounds, one can isolate the tSZ spectral shape to produce maps of the Compton- y parameter alone. The maps used in this work will be described in Section 2.

WHIM signal is generally very weak due to their low density and temperature, for this reason, detecting the signal from a single filament is challenging. An environment in which WHIM can be more easily detected is between merging galaxy clusters: as clusters gravitate towards each other, a primordial filament between them is compressed, increasing its pressure, and enhancing its tSZ and X-ray signal. A notable example is the Abell 399 – Abell 401 system, extensively studied using multi-wavelength observations from the X-rays to the radio-mm [9], that show the presence of a gas bridge connecting the two clusters. The morphology of the clusters is consistent with a pre-merger scenario, therefore, the filament between them is likely a primordial filament being compressed. Another interesting system, although more complex and perturbed, is the Abell 3391 – Abell 3395 cluster pair. Planck data could not firmly detect a bridge of gas between the clusters [9], however, X-ray data from eROSITA show an excess of gas between them [10], with a component of warm gas whose physical parameters are compatible with WHIM. However, observing WHIM between clusters at higher redshift is challenging, due to the forementioned low X-ray signal, and the lack of high resolution observations capable of disentangling clusters from filaments. A method that has been extensively used to probe the outskirts of clusters in search for faint WHIM signals is stacking. With this method, a large number of sky maps are aligned on clusters and then averaged together, increasing the signal-to-noise ratio of the final map and allowing for the

detection of weaker signals, although averaged over the cluster population. Different stacking approaches have been explored to probe the outskirts of clusters and filaments of the cosmic web. A first method, "pair stacking", consists in identifying pairs of interacting clusters and align their centers to the same stack coordinates thus only stacking the signal from filaments between the cluster centers. Examples of this method can be found in literature applied to Planck Compton- y maps [13–15]. In these works, the stacking was performed by aligning maps according to a catalog of proxy galaxies like red luminous galaxies (RLRGs) [14, 15] or CMASS galaxies [13], that typically trace halos of few $10^{13}M_{\odot}$. The same stacking procedure was also applied to X-ray data, like from ROSAT [16] or eROSITA [17], or to CMB lensing maps [13]. The combination of different datasets (i.e. SZ, X-rays or lensing) allows to break the degeneracy between temperature and gas density, thus allowing for a full characterization of WHIM. Another widely used and complementary technique is using filament finders like DisPerSE [18], that extract a catalog of filaments from a catalog of points in a 2D or 3D space, and then computes the radial profile [19, 20]. The catalog of points in space can be for instance the same catalog of LRGs or CMASS galaxies used for pair stacking. For this reason, this method usually probes halos in the $10^{13}M_{\odot}$ mass range. Except for the few notable examples mentioned before, there is no data for more massive systems, of the order of $10^{14}M_{\odot}$, that although being less common, might contain a significant amount of gas. In this work, we present a measurement of the Compton- y excess found between pairs of massive clusters extracted from a preliminary version the ACT-DR6 galaxy cluster catalog. This proceeding summarizes the results presented in Isopi *et al.* (2025) [21], with more focus on the results from the pair stacking.

2 ACT data: DR6 maps and cluster catalog

The Atacama Cosmology Telescope (ACT)¹ was a 6 m off-axis gregorian telescope located in Cerro Toco, Chile, at an altitude of 5190m. It observed between 2007 and 2022 with three generations of receivers based on transition edge sensors (TES): MBAC [22], ACTPol [23] and AdvACT [24], targeting a wide range of frequency, with science bands at 28, 39, 98, 150, 220 and 270 GHz. The latest receiver iteration, ACTPol, observed between 28 and 220 GHz with polarization capabilities. Results from ACT, including maps and products, are available on the LAMBDA website², in a series of data releases (DR1–6). The latest data release, DR6, comprises data collected between 2008 to 2022, and the resulting maps cover a sky area of 19000 square degrees with a median depth of $10 \mu\text{K}$ [25] and a resolution of $1\text{--}2'$ depending on the frequency band. Using an internal linear combination pipeline, component-separated maps of the CMB signal and of the Compton- y parameter were derived from ACT data co-added with Planck data for better foreground removal and recovery of the largest angular scales [27]. In this work, we use the Compton- y map described in [27], that covers about one third of the sky with varying depth, at a resolution of $1.6'$. Single frequency maps from ACT were used to build a catalog of blindly-detected galaxy clusters. A method based on a multi-frequency matched filter designed to maximize the signal-to-noise ratio on structures whose profile matches an universal pressure profile [29]. The resulting catalog, that is part of the ACT DR5 and available on LAMBDA, contains about 4000 blindly detected clusters over $12\,000 \text{ deg}^2$ of the sky [28]. The catalog used in this study is a preliminary version of the ACT DR6 cluster catalog, that contained about 7400 galaxy clusters [26]. In this catalog, we identify candidate cluster pairs by thresholding their projected sky distance, $d_{sky} < 10 \text{ Mpc}$ and their peculiar velocity difference along the line of sight, $\Delta v_z < 5000 \text{ km s}^{-1}$, that is the

¹<https://act.princeton.edu/>

²<https://lambda.gsfc.nasa.gov/>

same criteria used to identify cluster pairs in the DR5 catalog [28]. The catalog contains clusters in a redshift range $0.04 < z_{pair} < 1.25$, where z_{pair} is the mean redshift of the two components of each cluster system. The mean calibrated mass for the sample is $3.5 \times 10^{14} M_{\odot}$.

3 Pair stacking of ACT clusters

We now describe the procedure we adopt to stack the cluster pairs. From the full ACT-DR6 Compton- y map [27] we extract square cut-out maps centered on the average coordinates of the two clusters, the center coordinates of each are products of the ACT cluster catalog. Each cut-out has a side that is 10 times the angular separation of the two components of each pair. We then reproject the cut-outs from the original *plate-Carrée* projection to gnomonic projection. Finally we rotate the maps such that the the axis between the two clusters is parallel to the X axis, and rescale them such that the distance between the two clusters is fixed at 50 pixels, or $25'$. This distance was chosen because it is close to the average sky separation of the clusters, in order to keep the rescaling factor close to 1 for the majority of the systems. Finally, we reject clusters that are overlapping, i.e. the distance between the two components is less than the sum of their scale radius, $R_{500,1} + R_{500,2} < 2$, or clusters with only photometric z measurement available, because the resulting Δv_z uncertainty was comparable to the threshold itself, leading to false positives in the stack. The stacking is performed in Fourier space. We deconvolve each map with a $1.6'$ beam scaled by the rescaling factor, and then co-add them weighting by the noise level of each map and S/N of the clusters in each pair. After rejecting cluster pairs with the criteria described before, the final stack is composed of 86 cluster pairs. The result is shown in the left panel of Figure 1. To estimate the excess emission in the inter-cluster region, we perform a 2D Markov Chain Monte Carlo (MCMC) fit following a similar approach as Hincks *et al.* (2022) [12]. We model the clusters with a generalized Navarro Frenk & White (gNFW) profile [29] and the filament with a cylindrical- β model [11]. The best fit parameters are shown in Table 1. The measured filament amplitude is $A_{fil} = 7.24^{+2.48}_{-2.29} \times 10^7$ with a significance of 3.3σ , where the significance is estimated with the likelihood ratio. Additionally, we use the Akaike information criteria [12] to further confirm that a model including a bridge is preferred with respect to a model without a bridge, accounting for the increased parameters. We find $\Delta_{AIC} = 10.29$, which results in the model including a bridge being strongly preferred [12].

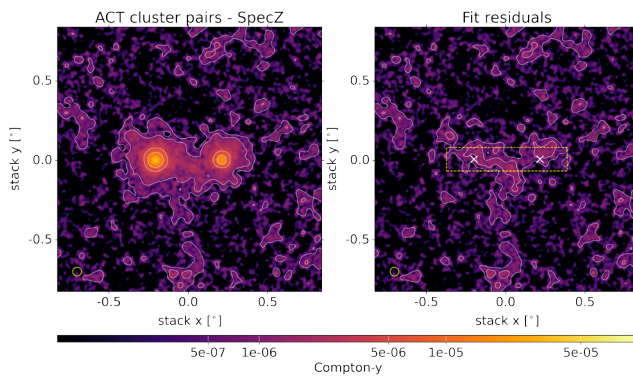


Figure 1. Left: stacked map of 86 ACT-selected cluster pairs. Right: the same stacked map, after subtracting the best fit gNFW profiles for the two clusters. The dashed box shows the best fit length l_{fil} and scale radius r_c of the filament. Source: [21]

Table 1. Best fit parameters for the stack shown in Figure 1

				Clusters parameters					
x_{c1} (px)	y_{c1} (px)	x_{c2} (px)	y_{c2} (px)	β_{c1}	β_{c2}	A_{c1} [$y \times 10^{-5}$]	A_{c2} [$y \times 10^{-5}$]	$r_{s,c1}$ [']	$r_{s,c2}$ [']
$38.23^{+0.04}_{-0.04}$	$63.32^{+0.04}_{-0.04}$	$88.25^{+0.04}_{-0.04}$	$63.24^{+0.04}_{-0.04}$	$3.32^{+0.10}_{-0.08}$	$3.13^{+0.15}_{-0.13}$	$6.08^{+0.15}_{-0.15}$	$3.66^{+0.18}_{-0.65}$	$1.53^{+0.08}_{-0.06}$	$1.29^{+0.10}_{-0.07}$
				Bridge parameters					
				l_{fil} [']	r_c [']	A_{fil} [$y \times 10^{-7}$]			
				$45.61^{+3.17}_{-9.61}$	$8.99^{+3.64}_{-0.98}$	$7.24^{+2.48}_{-2.29}$			

4 Discussion and conclusions

We measure an excess of Compton- y emission, that we interpret as the SZ signal produced by hot gas in filaments between the stacked clusters, of $A_{fil} = 7.24^{+2.48}_{-2.29} \times 10^7$ with a significance of 3.3σ . This excess is significantly larger (about an order of magnitude) compared to past stacking results obtained using Planck data [13–15]. Simulations show that a positive correlation exists between density ρ_{fil} and width D_{fil} of a filament and the mass of the halos embedded in them [30]. This implies that filaments associated with more massive halos will be denser, wider and hotter, thus their tSZ signal will be enhanced, and this is supported our finding of an higher Compton- y excess. Figure 2 shows a comparison between the measurement presented in this work and other literature measurements. The best fit slope, fitted only on the data points associated with pair stacking works, is $\alpha = 1.21^{+0.34}_{-0.35}$, that is compatible with the self-similar slope of clusters within 1.3σ , $\alpha_{cl} = 5/3$. Since filaments are not virialized, they do not show a self similar behaviour like clusters. Therefore, this relation should be considered as a qualitative scaling relation, possibly useful to estimate in advance the expected signal strength from a filament for targeted observations and proposals. However, although with limited data (since the only stacking result at high masses is the one we are presenting in this proceeding), this relation hint that the scaling relations observed in simulations exist.

The slope of the mass-amplitude relation for filaments will be interesting to study with more future data with higher sensitivity and resolution. Future survey observations from the Simons Observatory ³ and the proposed AtLAST telescope ⁴ will provide higher sensitivity, higher resolution Compton- y maps of the sky, allowing for a better characterization of interacting cluster systems, including resolved observations even at high redshift. For example, the Compton- y white noise sensitivity predicted for AtLAST is $\sigma_y \approx 2 \times 10^{-7}$, about an order of magnitude better than the current ACT Compton- y maps. We also stress the importance of combining multi-wavelength observations to fully characterize WHIM. Including X-ray data will be fundamental to give a reliable measurement of the electron temperature in these filaments, that in combination with the tSZ signal will provide an estimate of the baryon density embedded in environments well outside galaxy clusters.

References

- [1] G. Hinshaw, *et al.*, <https://arxiv.org/abs/1212.5226> (2012)
- [2] Planck Collaboration, <https://arxiv.org/abs/1807.06209> (2018)
- [3] ACT Collaboration, <https://arxiv.org/abs/2503.14452> (2025)
- [4] M. Fukujita, *et al.*, *Astrophys.J.*503:518 (1998)
- [5] R. Cen and J. P. Ostriker, *APJ*, Volume 514, Issue 1, pp. 1-6 (1999)

³<https://simonsobservatory.org/>

⁴<https://www.atlast.uio.no/>

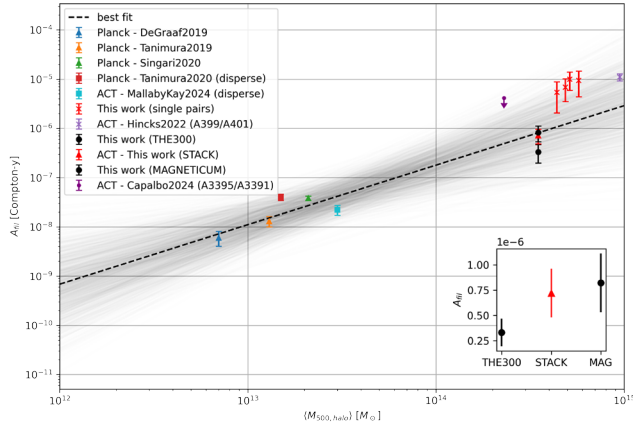


Figure 2. Compton- y excess due to filaments between stacked clusters plotted against the average mass of the stacked clusters. Source: [21]

[6] M. Birkinshaw, *Physics Reports*, Volume 310, Issue 2-3, p. 97-195. (1999)

[7] R. A. Sunyaev, *et al.*, *Comments on Astrophysics and Space Physics*, Vol. 4, p.173 (1972)

[8] Zeldovich, Ya. B., *et al.*, *Astrophysics and Space Science*, Volume 4, pp. 301-316 (1969)

[9] Planck Collaboration VIII, 10.1051/0004-6361/201220194, (2013)

[10] T. H. Reiprich, *et al.*, *AANDA*, Volume 647, id.A2, 30 pp. (2021)

[11] V. Bonjean, *et al.*, *AANDA*, Volume 609, id.A49, 11 pp. (2018)

[12] A. Hincks, *et al.*, *MNRAS*, Volume 510, Issue 3, pp.3335-3355 (2022)

[13] A. De Graaff *et al.*, *AANDA*, Volume 624, id.A48, 12 pp. (2019)

[14] H. Tanimura *et al.*, *MNRAS*, Volume 483, Issue 1, pp.223-234 (2019)

[15] B. Singari *et al.*, *JCAP*, Issue 08, article id. 028 (2020)

[16] H. Tanimura *et al.*, *MNRAS*, Volume 483, Issue 1, pp.223-234 (2019)

[17] H. Tanimura *et al.*, *AANDA*, Volume 667, id.A161, 10 pp., (2022)

[18] T. Sousbie, <https://arxiv.org/abs/1302.6221>

[19] H. Tanimura *et al.*, *MNRAS*, Volume 491, Issue 2 (2020)

[20] M. Mallaby-kay *et al.*, in preparation (2025)

[21] G. Isopi *et al.*, *JCAP*, Volume 2025, Issue 08, id.078, 43 pp. (2025)

[22] D. S. Swetz, *et al.*, *APJ Supplement*, Volume 194, Issue 2, article id. 41, 17 pp. (2011).

[23] K. T. Crowley, *et al.*, *SPIE Conference Series*, Vol 9914, article id. 991431 (2016).

[24] E. Grace, *et al.*, *SPIE Conference Series*, Vol 9153, article id. 915310 (2014)

[25] S. Naess, *et al.*, <https://arxiv.org/abs/2503.14451> (2025)

[26] ACT Collaboration, *et al.*, in prep (2025)

[27] W. Coulton, *et al.*, *Phys. Rev. D* 109, 063530, (2024)

[28] M. Hilton, *et al.*, *APJ Supplement*, Volume 253, Issue 1, article id. 3, 25 pp. (2021).

[29] D. Nagai, *APJ*, Volume 668, Issue 1, pp. 1-14 (2007)

[30] W. Zhu, *et al.*, *APJ*, Volume 967, Issue 2, id.141, 10 pp.